ELSEVIER

Journal of Power Sources 68 (1997) 646–651

JOURNAL OF POWER SOURCES

Comparative study of $Li[Li_xMn_{2-x}]O_4$ and LT-$LiMnO_2$ for lithium-ion batteries

Tsutomu Ohzuku *, Shinya Kitano, Masato Iwanaga, Hiroshi Matsuno, Atsushi Ueda

Electrochemistry and Inorganic Chemistry Laboratory, Department of Applied Chemistry, Faculty of Engineering, Osaka City University, Sugimoto 3-3-138, Sumiyoshi, Osaka 558, Japan

Accepted 14 October 1996

Abstract

A comparative study of $Li[Li_xMn_{2-x}]O_4$ and LT-$LiMnO_2$ for lithium-ion batteries was done in order to understand anomalous behavior of the Li–Mn–O ternary phases in terms of solid-state electrochemistry. Stoichiometric $LiMn_2O_4$ shows the largest capacity at 4 V versus Li while its rechargeable capacity fades rapidly. Conversely, nonstoichiometric $Li[Li_xMn_{2-x}]O_4$ (normally $0 < x < 1/3$ in assumed defect-spinel formulation) shows excellent rechargeability compared with stoichiometric $LiMn_2O_4$ although the rechargeable capacity monotonically decreases as x in $Li[Li_xMn_{2-x}]O_4$ increases, indicating a trade-off relation between cycleability and rechargeable capacity in applying this material to lithium-ion batteries. LT-$LiMnO_2$ shows rechargeable capacity of more than 150 mAh g^{-1} in voltages between 2.0 and 4.0 V after converting its structure to a cubic phase during the first charge. Differences and similarities between the two cubic (Li–Mn–O) phases are described and the specific problems in developing materials for lithium-ion batteries are discussed. © 1997 Elsevier Science S.A.

Keywords: Lithium-ion batteries; Manganese oxides; Rechargeability

1. Introduction

Electrochemistry and structural chemistry of manganese (di)oxide (MnO_2) in both aqueous and nonaqueous electrolyte is of great interest among electrochemists and battery researchers. Manganese (di)oxides, such as ramsdellite, pyrolusite, and the intergrowth products between them, can accommodate hydrogen ions (protons) and electrons forming manganese oxyhydroxides (groutite or manganite in its pure form), called a hydrogen ion (proton)–electron system [1]. The nonstoichiometric nature of manganese (di)oxide in terms of the Mn–O–H ternary phases has been widely recognized in addition to the poor crystallinity of battery-active manganese (di)oxide [2]. These manganese (di)oxides, especially electrolytic MnO_2 (EMD) and chemically prepared MnO_2 (CMD), can also accommodate lithium ions and electrons [3], called a lithium ion–electron system, so that they can also be used in nonaqueous lithium batteries. The structural relationship between Mn–O–H phases and Li–Mn–O phases can be seen in these MnO_2 compounds [3]. However, the nonstoichiometric nature of these MnO_2 compounds combined with their poor crystallinity prevents us to further develop solid-state electrochemistry of manganese dioxide [4,5].

λ-MnO_2 ($Fd\bar{3}m$) [6] shows such a unique character that it cannot be reduced to MnOOH in a topotactic manner in a proton–electron system, while it can be reduced to $LiMnO_2$ ($I4_1/amd$) in a topotactic manner in a lithium–electron system [7]. Crystallinity on a series of $\square MnO_2$($Fd\bar{3}m$)–$LiMn_2O_4$($Fd\bar{3}m$)–$LiMnO_2$($I4_1/amd$) is superior to those of other lithiated manganese (di)oxides [3–5,7].

In this paper we report a characteristic feature of nonstoichiometry in the Li–Mn–O ternary phases and discuss the specific problems in developing lithiated manganese (di)oxides for lithium-ion batteries.

2. Experimental

The Li–Mn–O ternary phases were prepared from MnOOH (manganite) and LiOH. A mixture of MnOOH and LiOH (molar ratio of Li/Mn; 0.5 to 2) was pressed into pellets (23 mm diameter and ~5 mm thickness) and precalcined under air or nitrogen stream typically at 600 °C for 12 h. The precalcined mixture was then ground, pressed into pellets again, and reacted in air or nitrogen at several temperatures. LT-$LiMnO_2$ was prepared by a method described in Ref. [8].

* Corresponding author.

PII S0378-7753(96)02573-6

The reaction products were ground and stored in a desiccator over blue silica gel and used for electrochemical tests without washing with distilled water. LT-$LiMnO_2$ supplied by Sedema was also used as received. The electrolyte used was 1 M $LiClO_4$ dissolved in propylene carbonate. Aluminum foil was mainly used as a current collector. In preparing the cathode, polyvinylidene fluoride (PVDF) dissolved in *N*-methylpyrrolidone (NMP) or polystyrene-block-poly(ethylene/butylene)-block-polystylene rubber (Kraton G1650, Shell Chemical) in toluene was used. A black viscous slurry was painted on the aluminum foil (1.5 cm × 2 cm). The prepared cathodes were dried under vacuum at 100 °C for more than 15 h prior to use. All procedures for handling and fabricating the electrochemical cells were performed in an argon-filled glove box. Other sets of experimental conditions are given in Section 3.

3. Results and discussion

During the past six years we have intensively examined the Li–Mn–O ternary phases in compositions ranging from Li/Mn = 1/4 in molar ratio ($Li_{1/4}MnO_2$) to Li/Mn = 2/1 (Li_2MnO_3) via Li/Mn = 1/1 ($LiMnO_2$), prepared at several temperatures from 200 to 1000 °C [9]. In the course of such systematic studies on lithiated manganese (di)oxides we recognized the nonstoichiometric nature of the Li–Mn–O ternary phases, which led to the discovery of LT-$LiMnO_2$ [8] following lithiated manganese (di)oxides [10,11] for rechargeable lithium batteries. Single cubic phases in terms of powdered X-ray diffraction (XRD) analysis can be prepared in compositions of Li/Mn = 1/2 to 4/5 at temperatures lower than 750 °C in air. Higher heating temperatures than that value result in phase separation from a cubic phase to $LiMn_2O_4$ and Li_2MnO_3. A critical temperature exists somewhere around 850 °C [12–14]. For this reason it was very difficult to prepare stoichiometric $LiMn_2O_4$ giving analytical values, such as Li wt.%, Mn wt.%, MnO_2 wt.%, and x in MnO_x, as close to the calculated values for stoichiometric $LiMn_2O_4$ [7], i.e., 3.84 (Li wt.%), 60.77 (Mn wt.%), 72.12 (MnO_2 wt.%), and 1.750 (x in MnO_x).

Fig. 1 shows the XRD patterns of the Li–Mn–O ternary phases selected in order to compare with respect to line shapes and location. All diffraction lines can be indexed assuming a cubic lattice. Samples in Fig. 1 (a)–(c) were prepared by heating a reaction mixture of MnOOH and LiOH at 750 °C in air. Molar ratios in Li/Mn were given in values loaded to prepare samples, not analytical values of these samples. As seen in Fig. 1 (a)–(c), one cannot distinguish each other unless careful structural analysis has been done. In general, higher lithium-ion concentrations give smaller cubic lattice constants. If we assume a defect-spinel formulation of $Li[Li_xMn_{2-x}]O_4$, x-values are calculated to be $x = 0$, 0.125, and 0.33 for (a), (b), and (c), respectively, in Fig. 1. The sample in Fig. 1(d) was prepared by the electrochemical oxidation of LT-$LiMnO_2$ up to 229 mAh g^{-1}. This sample

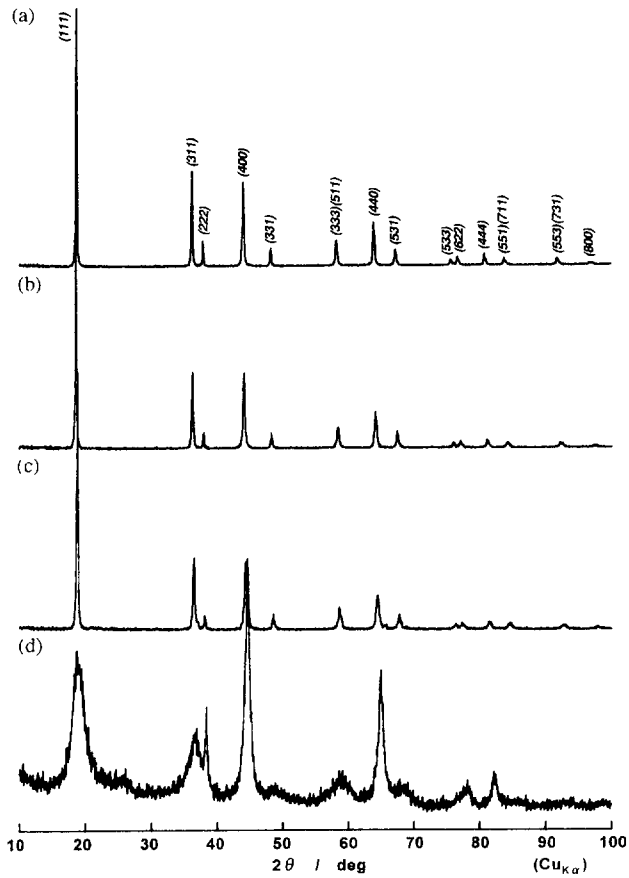

Fig. 1. XRD patterns of the Li–Mn–O ternary phases prepared by heating a reaction mixture of MnOOH and LiOH at 750 °C in air. Molar ratios of Li/Mn are (a) Li/Mn = 1/2, (b) 3/5, and (c) 4/5. XRD pattern of the sample prepared by the electrochemical oxidation of LT-$LiMnO_2$ up to 229 mAh g^{-1} is also shown in (d). Miller indexes are given assuming a cubic lattice. The lattice constant is calculated to be (a) $a = 8.23(9)$ Å, (b) $a = 8.20(8)$ Å, (c) $a = 8.17(2)$ Å, or (d) $a = 8.11(9)$ Å

can also be indexed assuming a cubic lattice [15–17], while diffraction lines are much broader than those of (a), (b), or (c) in Fig. 1.

Fig. 2 shows the charge and discharge curves of the Li–Mn–O phases prepared from MnOOH and LiOH. As seen in Fig. 2, rechargeable capacity of the sample (shown in (a)) whose composition is close to stoichiometric $LiMn_2O_4$ fades rapidly in comparing with other samples in (b), (c), or (d). The x-values in $Li[Li_xMn_{2-x}]O_4$ are calculated to be $x = 0$,0.10, 0.175, and 0.333 for (a), (b), (c), and (d), respectively, in Fig. 2. If the defect-spinel formulation of $Li[Li_xMn_{2-x}]O_4$ is properly worked out, an x-value of 0.33 means $Li[Li_{1/3}Mn_{5/3}]O_4$, thus only containing tetravalent manganese ions in a solid matrix, so that zero rechargeable capacity at 4 V is expected. However, 40–60 mAh g^{-1} of rechargeable capacity at 4 V can usually be observed in these samples.

Fig. 3 shows the change in lattice dimension as a function of x in $Li[Li_xMn_{2-x}]O_4$ calculated from the molar ratio of Li/Mn loaded to prepare samples. Triangles in Fig. 3 indicate the lattice dimensions for an oxidized form of

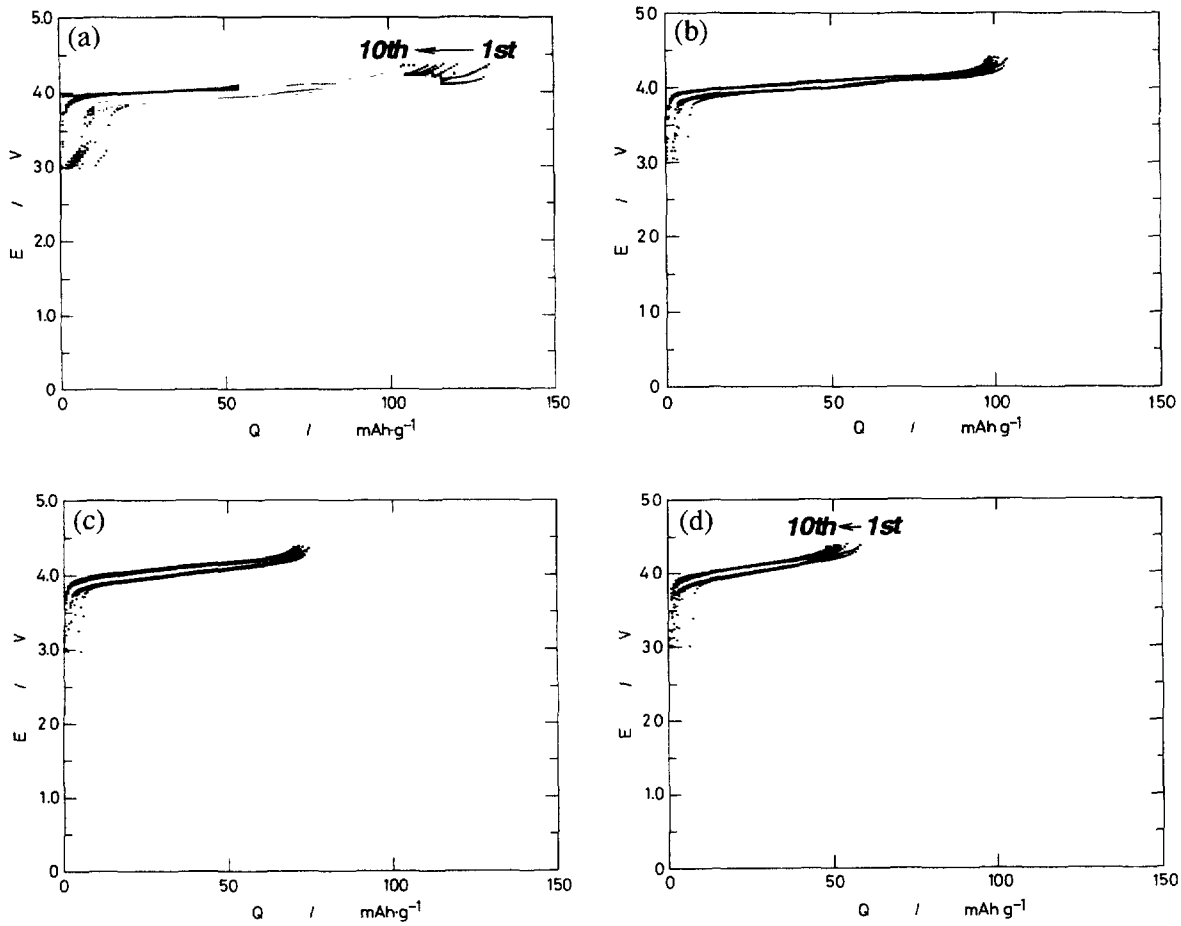

Fig. 2. Charge and discharge curves of the Li–Mn–O ternary phases, prepared from MnOOH and LiOH, at voltages between 3.0 and 4.4 V at a current density of 0.10 mA cm^{-2} in 1 M $LiClO_4$, PC at 30 °C. The x-values in $Li[Li_xMn_{2-x}]O_4$ formulation are (a) $x=0$, (b) $x=0.1$, (c) $x=0.175$, and (d) $x=0.333$. The positive electrode consists of 85 wt.% $Li[Li_xMn_{2-x}]O_4$, 10 wt.% acetylene black and 5 wt.% Kraton G.

$Li[Li_xMn_{2-x}]O_4$ prepared by potentiostatic oxidation of the samples at 4.35 V versus Li for 12 h. As seen in Fig. 3, the lattice dimension of $Li[Li_xMn_{2-x}]O_4$ monotonically decreases as x increases. Conversely, the lattice dimension of the oxidized form of $Li[Li_xMn_{2-x}]O_4$ increases as x increases up to about 0.2 and then it levels off at ~8.10 Å. Consequently, the change in lattice dimension during charge and discharge is getting small as x increases. This may give a beneficial effect upon capacity retention by cycling [18–20], but this is a trade-off between cycleability and rechargeable capacity.

The solid-state redox reaction of stoichiometric $LiMn_2O_4$ is known to be a topotactic reaction consisting of a cubic-cubic two-phase reaction ($a=8.04(5)$ and $8.14(2)$ Å) and a single phase reaction in a cubic phase ($a=8.14(2)$ to $8.23(9)$ Å) [7] for the 4 V region under consideration. It should be noted that cubic phases having the lattice dimensions between $a=8.04$ Å and $a=8.14$ Å cannot be found due to a topotactic two-phase reaction for stoichiometric $LiMn_2O_4$. However, the lattice dimensions of the oxidized form of $Li[Li_xMn_{2-x}]O_4$ are in that range as seen in Fig. 3.

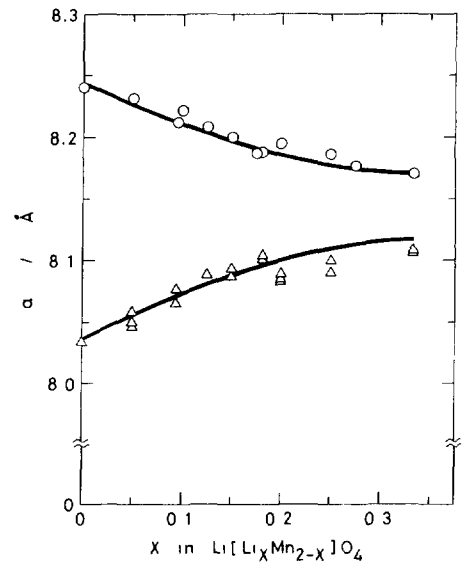

Fig. 3. Change in cubic lattice dimension as a function of x in $Li[Li_xMn_{2-x}]O_4$. Open circles (○) indicate the lattice constant of $Li[Li_xMn_{2-x}]O_4$ prepared from MnOOH and LiOH at 750 °C in air. Triangles (△) indicate the lattice constants of an oxidized form prepared by potentiostatic oxidation of $Li[Li_xMn_{2-x}]O_4$ at 4.35 V vs. Li for 12 h.

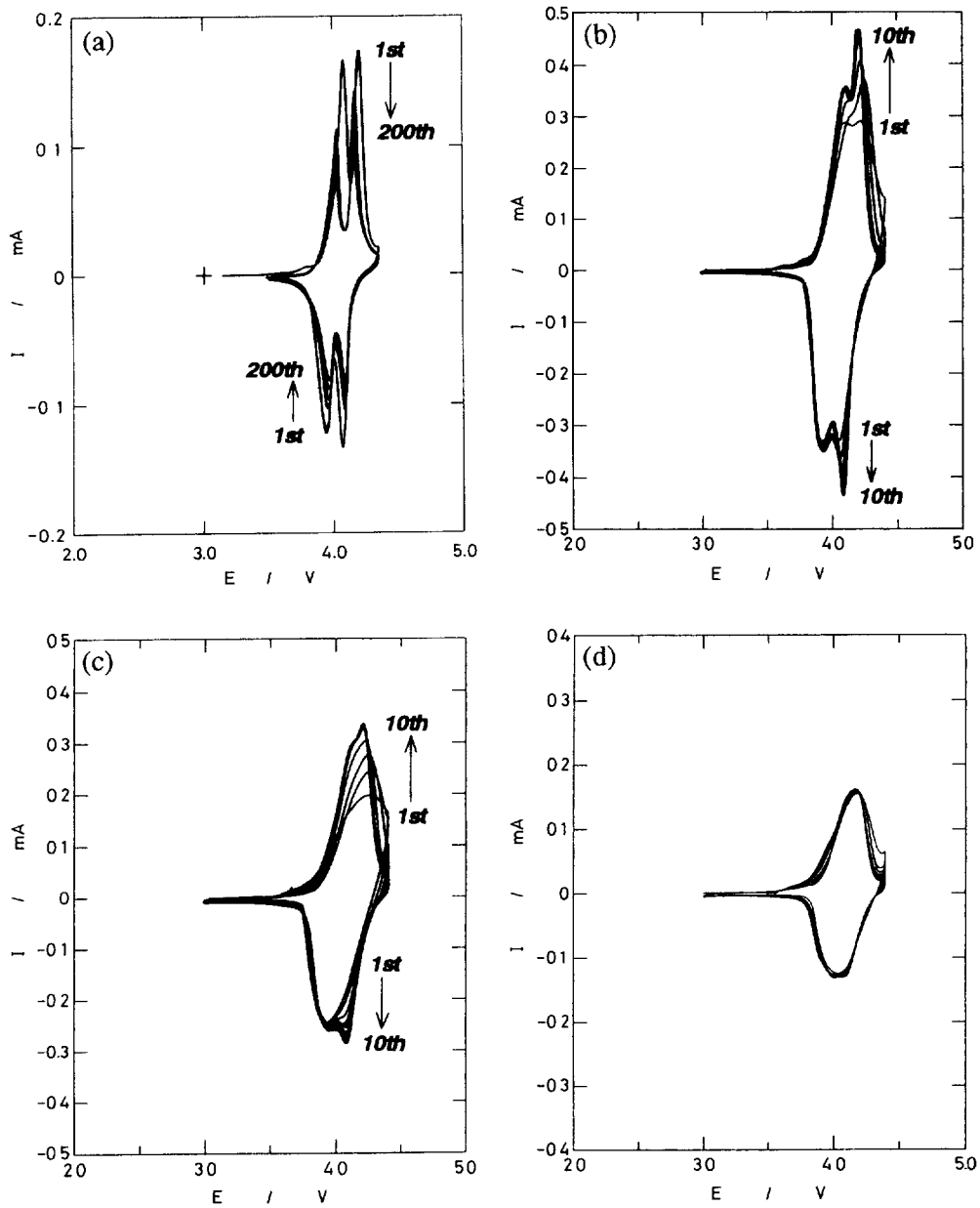

Fig. 4. Slow scan cyclic voltammograms for Li/Li[Li_xMn_{2-x}]O_4 cells at voltages between 3.0 and 4.4 V at a scan rate of 0.1 mV s^{-1}; (a) $x=0$, (b) $x=0.1$, (c) $x=0.175$, and (d) $x=0.333$. The electrode consisted of 60 wt % Li[Li_xMn_{2-x}]O_4, 35 wt % acetylene black, and 5 wt % Kraton G

In order to examine whether or not the electrochemical reaction of Li[Li_xMn_{2-x}]O_4 is the same as that of stoichiometric $LiMn_2O_4$, slow scan cyclic voltammetry of these samples was carried out. The results are shown in Fig. 4. The cells were cycled many times until the steady-state voltammetric profiles were obtained. Stoichiometric $LiMn_2O_4$ clearly shows two redox couples characterized by 3.95 and 4.11 V of midpoint voltages between each anodic and cathodic peak. These peaks gradually change in their shapes from well-defined two humps to rounded or broadened single hump as x in Li[Li_xMn_{2-x}]O_4 increases. For $x=0.10$ or 0.175 in Fig. 4, the peaks were gradually shaped up by cycling, suggesting the change in structural order which could not be identified by XRD.

The movement of transition metal ions in a close-packed oxygen array is normally unfavorable to materials based on a topotactic reaction. Accordingly, it is quite unusual that mobile transition metal ions in a solid matrix play an important role in determining rechargeability for lithium-ion batteries. Fig. 5 shows the charge and discharge curves of LT-$LiMnO_2$. The starting material of LT-$LiMnO_2$ has an orthorhombic lattice (space group: $Pm2m$, $a=2.80(6)$ Å, $b=5.74(8)$ Å, $c=4.57(3)$ Å), called a zigzag-layered structure. In LT-$LiMnO_2$ all of the octahedral sites in a cubic close-packed oxygen array are occupied by either manganese or lithium ions. During the first charge, the orthorhombic phase is entirely destroyed and converted to a cubic phase as shown in Fig. 1(d), indicating that trivalent or tetravalent manga-

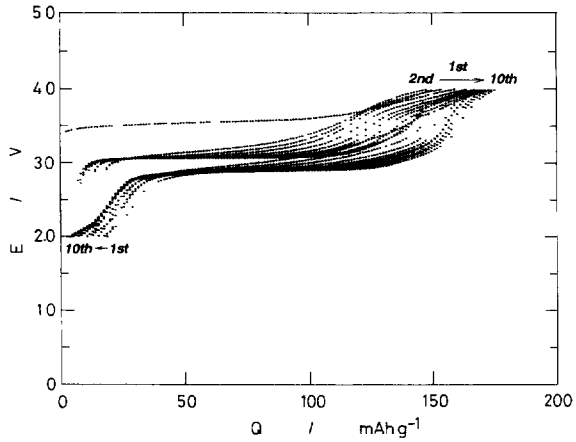

Fig 5. Charge and discharge curves for an Li/LT-$LiMnO_2$ cell operated at voltages between 2 0 and 4 0 V at a current density of 0 17 mA cm^{-2} at 30 °C. The electrolyte used was 1 M $LiClO_4$/PC. The electrode consisted of 80 wt.% LT-$LiMnO_2$, 10 wt % acetylene black, and 10 wt % PVDF

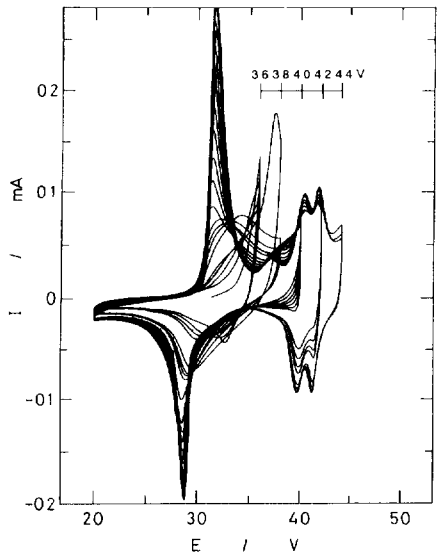

Fig. 6. Slow scan cyclic voltammograms for an Li/LT-$LiMnO_2$ cell at a scan rate of 0.1 mV s^{-1} at 30 °C The lower voltage was fixed to be 2 0 V and upper voltages were set stepwise by a 0.2 V increment from 3.6 to 4.4 V The electrode consisted of 60 wt.% LT-$LiMnO_2$, 35 wt.% acetylene black, and 5 wt.% PVDF

nese ions at the octahedral sites can move from one site to another, like lithium ions can do, in a cubic close-packed oxygen array in order to stabilize a solid matrix. The situation observed for the electrochemical reaction of LT-$LiMnO_2$ is quite different from those observed for topotactic reactions of many □MeO_2 or $LiMeO_2$ compounds [21], where Me denotes a transition metal element and □ indicates a vacant octahedral site.

A striking feature of LT-$LiMnO_2$ is that the solid-state redox reaction is adjustable by the voltage applied to the material. Fig. 6 shows the results on the window-opening experiments for slow scan cyclic voltammetry of LT-$LiMnO_2$ by a stepwise increment of 0.2 V from 3.6 to 4.4 V. The built-up curves of LT-$LiMnO_2$ from inactive to active behavior, depending on the voltage window, can be seen in Fig. 6. XRD

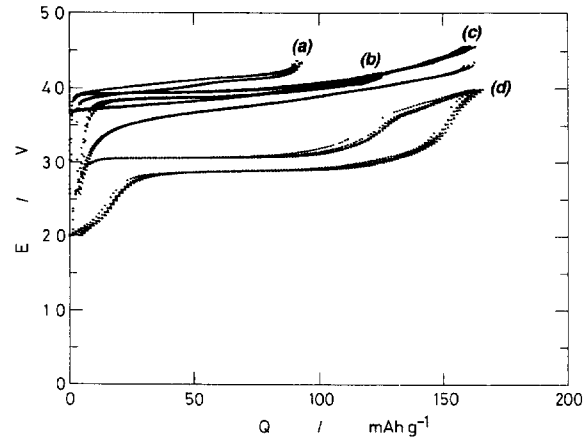

Fig 7. Charge and discharge curves of candidate materials for positive electrode use in lithium-ion batteries: (a) $Li[Li_{1/8}Mn_{15/8}]O_2$ (a defect-spinel formulation assumed); (b) $LiCoO_2$, (c) $LiAl_{1/4}Ni_{3/4}O_2$, and (d) LT-$LiMnO_2$.

results (not shown) indicate the reversible reaction proceeds as a cubic phase for both the 3 V and the 4 V regions, while the electrochemical behavior of LT-$LiMnO_2$ looks similar to that of stoichiometric $LiMn_2O_4$, not $Li[Li_xMn_{2-x}]O_4$.

Fig. 7 shows the results on the Li–Mn–O ternary phases for lithium-ion batteries, in which $LiCoO_2$ and $LiAl_{1/4}Ni_{3/4}O_2$ are also shown by comparison. As seen in Fig. 7, the Li–Mn–O ternary phases can be used as positive electrodes for both the 3 V and the 4 V lithium-ion batteries. Of these, stoichiometric $LiMn_2O_4$ and its derivatives show the highest operating voltage among insertion materials [21] reported so far for lithium-ion batteries.

Acknowledgements

The authors thank Dr J.C. Rousche, Sedema, for supplying LT-$LiMnO_2$. The present work was partly supported by a grant-in-aid for Scientific Research from the Ministry of Education, Science and Culture, Japan.

References

[1] T. Hirai, I. Tari and T. Ohzuku, *Yohyuen, 26* (1983) 265.
[2] *Manganese Dioxide Symp., 1* (1975); *2* (1980).
[3] T Ohzuku, M. Kitagawa and T. Hirai, *J Electrochem. Soc., 136* (1989) 3169.
[4] T. Ohzuku, M. Kitagawa and T. Hirai, *J Electrochem Soc., 137* (1990) 40.
[5] T. Ohzuku, J. Kato, K. Sawai and T Hirai, *J. Electrochem. Soc., 138* (1991) 2556.
[6] J.C. Hunter, *J Solid State Chem., 39* (1981) 142.
[7] T. Ohzuku, M Kitagawa and T. Hirai, *J Electrochem. Soc., 137* (1990) 769.
[8] T. Ohzuku, A. Ueda and T. Hirai, *Chem. Express, 7* (1992) 193.
[9] A. Yamamoto, *M.S. Thesis*, Osaka City University, 1992.
[10] T. Ohzuku, K. Sawai and T. Hirai, *Chem Express, 4* (1989) 777
[11] T. Ohzuku, K Sawai and T. Hirai, *The Electrochemical Society Softbounded Proc. Ser.*, Vol. 91-3, Pennington, NJ, USA, 1991, pp 318–325.

[12] A. Ueda, K. Furukawa and T. Ohzuku, *Ext. Abstr., 34th Battery Symp. Japan, Hiroshima, Nov. 1993*, pp. 35–36.
[13] J.M. Tarascon, W.R. McKinnon, F. Coowar, T.N. Bowmer, G. Amatucci and D. Guyomard, *J. Electrochem. Soc., 141* (1994) 1421.
[14] Y. Gao and J.R. Dahn, *J. Electrochem. Soc., 143* (1996) 100.
[15] T. Ohzuku, A. Ueda and K. Furukawa, *Ext. Abstr. 33rd Battery Symp. Japan, Tokyo, Sept. 1992*, pp. 15–16.
[16] J.M. Reimers, E.W. Fuller, E. Rossen and J.R. Dahn, *J. Electrochem. Soc., 140* (1993) 3396
[17] R.J. Gummow and M.M. Thackeray, *J. Electrochem. Soc., 141* (1994) 1178.
[18] J.M. Tarascon, D. Guyomard and G.L. Baker, *J. Power Sources, 43–44* (1993) 689.
[19] V. Manev, A. Momchilov, A. Nassalevska and A. Kozawa, *J. Power Sources, 43–44* (1993) 551.
[20] Y. Xia and M. Yoshio, *J. Electrochem. Soc., 143* (1996) 825
[21] T. Ohzuku and A. Ueda, *Solid State Ionics, 69* (1994) 201.